1626-A

Setting of a Magmatic Sulfide Occurrence in a Dismembered Ophiolite, Southwestern Oregon

NEWARK PUBLIC LIBRARY

APR 3 1986

U. S. GOVT. PUBS.
DEPOSITORY 376

U.S. GEOLOGICAL SURVEY BULLETIN 1626–A

I 19. 3:

READEX MICRO best copy available

Chapter A

Setting of a Magmatic Sulfide Occurrence in a Dismembered Ophiolite, Southwestern Oregon

By MICHAEL P. FOOSE

A reporting of an unusual occurrence of magmatic sulfides in part of an ophiolite

U.S. GEOLOGICAL SURVEY BULLETIN 1626
CONTRIBUTIONS TO THE GEOLOGY OF MINERAL DEPOSITS

DEPARTMENT OF THE INTERIOR
DONALD PAUL HODEL, Secretary

U.S. GEOLOGICAL SURVEY
Dallas L. Peck, Director

UNITED STATES GOVERNMENT PRINTING OFFICE: 1986

For sale by the Distribution Branch, U.S. Geological Survey,
604 South Pickett Street, Alexandria, VA 22304-4658

Library of Congress Cataloging-in-Publication Data

Foose, M. P.
Setting of a magmatic sulfide occurrence in a dismembered ophiolite, southwestern Oregon.

(Contributions to the geology of mineral deposits) (U.S. Geological Survey bulletin ; 1626-A)
Bibliography: p. 21
Supt. of Docs. no.: I 19.3L1626-A)
1. Sulphides. 2. Rocks. Igneous—Oregon. 3. Ophiolites—Oregon. 4. Pyroxenite—Oregon. I. Title. II. Series. III. Series: U.S. Geological Survey bulletin ; 1626-A.
QE75.B9 no. 1626-A 557.3 s [553.6'68] 85-600137
[QE389.2]

CONTENTS

Abstract **A1**
Introduction **A1**
Regional geology **A1**
Previous work **A3**
Sulfide occurrence **A3**
Lithology **A4**
  Pyroxene cumulates **A4**
  Metagabbroic sequence **A6**
Mineral and rock analyses **A8**
Geothermometry and metamorphism **A15**
Summary and discussion **A16**
References cited **A21**

FIGURES

1. Index map and generalized geologic setting of the Illinois River sulfide occurrence **A2**
2. Geology of the Illinois River sulfide occurrence **A4**
3. Photomicrographs of sulfides in pyroxenite **A7**
4. Plot of pyroxene compositions in the Ca-Mg-Fe ternary **A11**
5. Chondrite-normalized plot of PGM and Au contents after recalculation to 100 percent sulfides **A20**
6. Composition of sulfides from cumulus pyroxenite plotted on the Fe-Ni-S diagram **A21**

TABLES

1. Modal compositions of rock units **A6**
2–11. Electron microprobe analyses of:
  2. Clinopyroxene **A9**
  3. Orthopyroxene **A10**
  4. Olivine **A12**
  5. Plagioclase **A13**
  6. Amphibole **A14**
  7. Cordierite **A15**
  8. Pentlandite **A15**
  9. Pyrrhotite **A16**
  10. Chalcopyrite **A17**
  11. Pyrite **A18**
12–13. Compositions of five sulfide-bearing samples:
  12. Whole-rock analyses **A19**
  13. Analyses recalculated to 100 percent sulfide **A19**
14. Metal-metal and metal-sulfur ratios from recalculated 100 percent sulfide compositions **A20**

Setting of a Magmatic Sulfide Occurrence in a Dismembered Ophiolite, Southwestern Oregon

By Michael P. Foose

Abstract

Cumulus pyroxenites are in fault contact with a sequence of predominantly metagabbroic rocks in southwestern Oregon. The cumulates are a relatively undeformed and unmetamorphosed series of rocks that are part of a dismembered ophiolite, and they host small amounts of sulfide minerals that are predominantly pyrrhotite and lesser amounts of chalcopyrite and pentlandite. Inclusions of sulfide globules in cumulus silicate grains show that an immiscible sulfide liquid was present while cumulus grains were precipitating. This sulfide liquid is estimated to have a Ni/Cu ratio of 0.2 and a chondrite normalized precious-metal pattern that is characteristic of sulfide deposits formed from gabbroic melts. The immiscible sulfide liquid formed a solid solution of $(Fe, Ni)_{1-x}S$ (Mss) and Fe-Cu-S (Iss); pentlandites crystallized from the Mss contain about 6 weight percent cobalt. In contrast, the metagabbroic rocks form a highly deformed, granulite-grade metamorphic complex and host a distinctly different sulfide assemblage composed of stringers of pyrite and lesser amounts of chalcopyrite.

Both types of sulfides have locally been mobilized along the faults that separate the two rock types. Mobilized pyrrhotite-rich sulfides from the pyroxenite form stringers in the fault and have been injected into metagabbro. In addition, these mobilized sulfides show lower contents of Ni, Co, Cu, and precious metals than do the sulfides that appear not to have moved, and they also contain pentlandite, which has between 16 to 28 weight percent Co.

Sulfides precipitated from crystallizing mafic and ultramafic magmas are not commonly reported in ophiolites, so these sulfides are a rare occurrence. Other concentrations of similar sulfides are present in this ophiolite, and thus there is a slight chance that larger and more economically attractive sulfide concentrations may be present. This occurrence is also of interest as it may represent the type of primary metal concentration which elsewhere in the world has been mobilized during shearing and serpentinization to form the Co-Ni-Cu vein deposits found in many altered ophiolites.

INTRODUCTION

A thrust slice of ultramafic and mafic igneous rocks, 20 km long by 6 km wide, is located near the Illinois River in southwestern Oregon (fig. 1). It is composed principally of harzburgite-dunite tectonite, cumulus pyroxenite, and sheared and metamorphosed gabbro. The ultramafic part of this complex is similar in petrology, structural fabric, and regional setting to several adjacent ultramafic bodies that have been identified as parts of Mesozoic ophiolites (Harper, 1980; Loney and Himmelberg, 1976, 1977; Himmelberg and Loney, 1973; Irwin, 1977). Although lacking the complete ophiolite sequence, probably these ultramafic rocks also represent part of a Mesozoic ophiolite complex and are a fragment of oceanic crust emplaced during the Nevadan orogeny (Coleman, 1972; Page, Gray, and others, 1981).

The cumulus pyroxenites and wehrlite in this thrust slice are similar to the cumulus sequences described from many other ophiolites (for example, Coleman, 1977; George, 1978; Jackson and others, 1975; Harper, 1979, 1980; Laurent, 1977; Morgan, 1977; Evarts, 1977; Hopson and Frano, 1977). They are therefore considered to represent rocks that accumulated on tectonized harzburgite and dunite, which may be either the depleted residuum left after partial melting (Dick, 1977; Coleman, 1977) or an earlier sequence of cumulates that were deformed during syncrystallization and subsolidus deformation (Thayer, 1980). The local occurrence of magmatic sulfides within cumulus pyroxenites in this thrust, however, represents an additional feature that either is not commonly found in other ophiolites or has not been reported.

This study concerns one small occurrence of copper-nickel-cobalt-bearing sulfides. Other similar occurrences of sulfides are found elsewhere within this thrust slice (Page, Gray, and others, 1981) and appear to be a common feature of this fragment of oceanic crust.

REGIONAL GEOLOGY

The mafic and ultramafic rocks associated with the Illinois River sulfide occurrence lie near the western boundary of the Klamath Mountains (fig. 1). Rocks immediately to the east of this boundary are part of the western Jurassic belt, the westernmost, structurally lowest, and youngest of four major thrust slices that make up the Klamath Mountains in this part of Oregon (Irwin, 1964, 1966). This package of rocks has been thrust westward over the younger coastal belt, which contains the Coast Range ophiolites and related eugeoclinal assemblages of the Dothan Formation and the correlative Franciscan assemblage (Bailey and others, 1970; Irwin, 1977). Although entirely

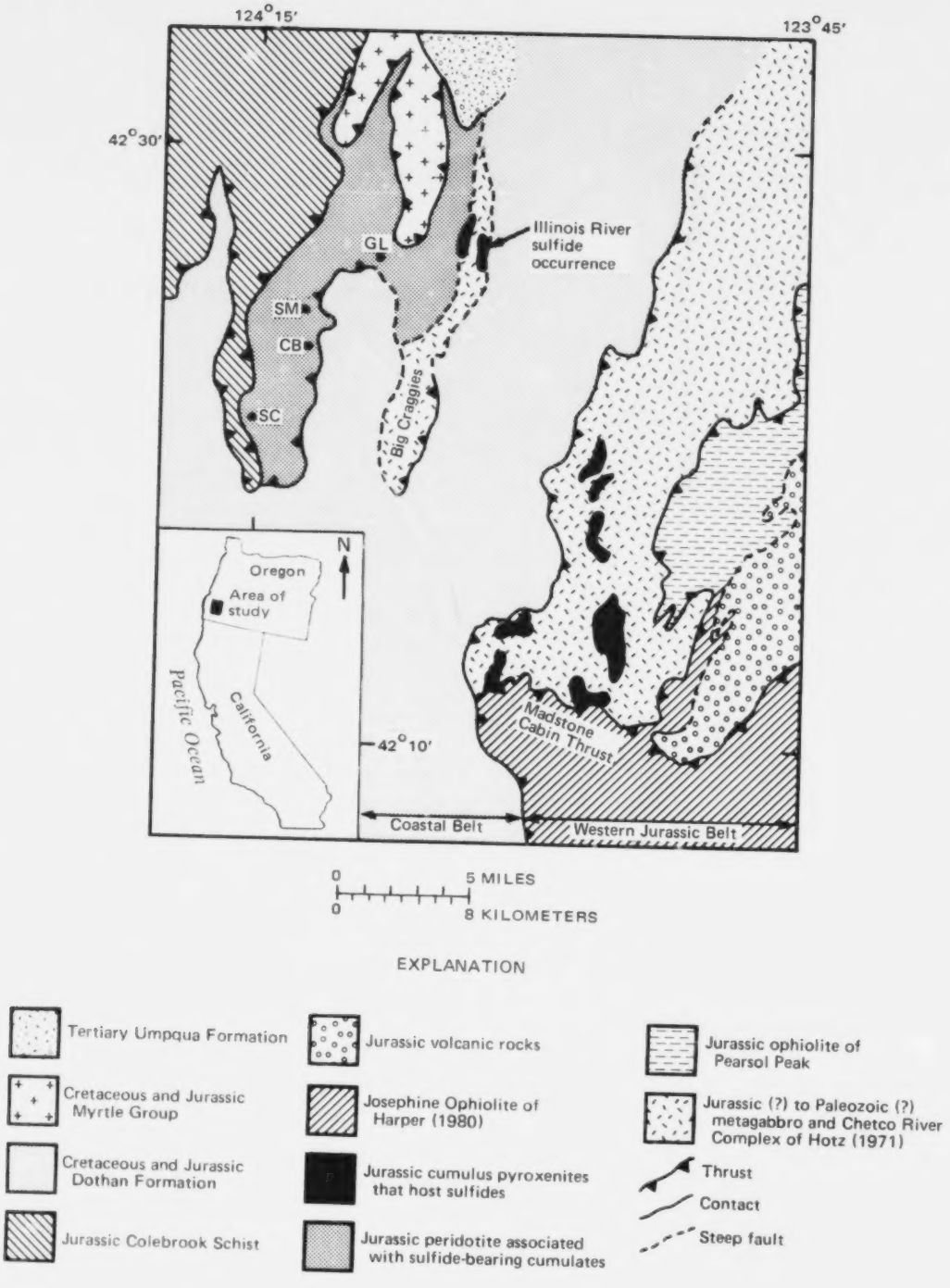

Figure 1. Index map and generalized geologic setting of the Illinois River sulfide occurrence. Geology modified from Coleman (1972), Ramp and others (1977), Garcia (1979), and Page, Gray, and others (1981). SC, Snow Camp Mountain; CB, Collier Butte; SM, Saddle Mountain; and GL, Game Lake.

surrounded by coastal-belt rocks, the thrust slice containing the Illinois River sulfide occurrence is made up of rocks that have both lithologic characteristics and isotopic ages similar to those found in parts of the adjacent western Jurassic belt. For these reasons, Irwin (1977) interpreted this thrust slice to be an outlier of the older Klamath Mountains.

Thrusts and steeply dipping faults divide the region around the sulfide occurrence into several structurally and lithologically distinct areas (fig. 1). The structurally lowest unit is the Dothan Formation, which is a flysch sequence composed predominantly of graywackes and mudstones (Diller, 1907; Ramp, 1969, 1975; Coleman, 1972; Page, Gray, and others, 1981) and which is overridden by four slices of mafic and ultramafic rocks and by several sheets of predominantly volcanic and sedimentary rocks. To the west are the peridotites, pyroxenites, and metagabbroic rocks with which the sulfides are associated. These, in turn, have been covered by thrust slices of Upper Jurassic deep-ocean sediments, the Colebrooke Schist, and conglomerates and rhythmically layered sandstones and mudstones of the Myrtle Group (Coleman, 1972); parts are also overlain by the Tertiary conglomerate deposits of the Umpqua Formation. To the east, the Dothan is overridden by the predominantly gabbroic rocks that make up the Chetco River complex of Hotz, 1971 (see also Ramp, 1975; Page, Gray, and others, 1981). The Chetco River complex is in turn covered by the steeply dipping harzburgites and dunites that have become known informally as the ophiolite of Pearsol Peak (Page, Gray, and others, 1981). Both the Chetco River complex and the ophiolite of Pearsol Peak are bounded on the east by steep faults, across which is a melange of volcanic rocks that probably correlate with Jurassic volcanic-arc deposits of the Galice and Rogue Formations (Garcia, 1979; Page, Gray, and others, 1981). Finally, the Chetco River complex, ophiolite of Pearsol Peak, and the volcanic rocks are overridden along the Madstone Cabin thrust by the Josephine Peridotite, which is part of the Josephine ophiolite of Harper (1980) and which is at least 157 m.y. old (Harper and Saleeby, 1980).

Ultramafic rocks in the area were emplaced along the western edge of the Jurassic continental margin during the Nevadan orogeny (Burchfiel and Davis, 1975). West-directed thrusting moved these sheets over the Chetco River complex, which includes rocks that may be part of a Late Jurassic subvolcanic island-arc complex (Nicholson, 1981) and volcanic rocks that are interpreted to be upper level volcanic-arc deposits (Garcia, 1979). Because the peridotites are also cut by numerous Late Jurassic intrusive bodies, it is possible that they either formed near an active arc complex (Harper, 1980) or were thrust onto an active arc system (Dick, 1977). Thrusting continued into the Cretaceous (Irwin, 1964) and later moved these rocks over the younger coastal-belt sequences. Much of the region was affected by normal faults formed during later Tertiary uplifts.

PREVIOUS WORK

Several studies have described the geology and mineral resources of the area near the Illinois River sulfide occurrence (Wells and others, 1949; Coleman, 1972; Ramp, 1975; Ramp and others, 1977; Page, Moring, and others, 1981; Page, Gray, and others, 1981). K-Ar ages from associated dioritic or gabbroic rocks near Saddle Mountain (Dott, 1965) indicate that peridotites near the sulfides probably formed about 285 m.y. ago. Diorites that crosscut peridotites near Game Lake and Collier Butte yield K-Ar ages of 139–145 m.y. (Dott, 1965; Coleman, 1972). Medaris (1972) and Henry and Medaris (1980) used pyroxene and pyroxene-spinel geothermometers to show that peridotites near Snow Camp Mountain have undergone recrystallization in the range of 1,200° to 900°C.

The diverse gabbroic rocks associated with the Illinois River sulfide occurrence and the adjacent and presumably related Chetco River complex include sheared and metamorphosed gneisses, rocks with well-developed cumulus textures, and hornblende-rich crosscutting intrusions (Hotz, 1971; Coleman, 1972; Ramp and others, 1977; Nicholson, 1981). K-Ar ages range from 285 to 215 m.y. (Hotz, 1971; Floyd Gray, oral commun., 1981) to between 140 and 151 m.y. (Hotz, 1971; Coleman, 1972; R.W. Tabor, *in* Himmelberg and Loney, 1973; Page, oral commun., 1981) and indicate a complex history of deformation and magmatism. Cumulus pyroxenites that have magmatic sulfides similar to those studies in this report occur as inclusions within younger gabbroic intrusions in part of the Chetco River complex (Loney and Himmelberg, 1977; Gray, 1980, and oral commun., 1980; Page, Gray, and others, 1981).

The sulfide occurrence studied here was previously identified as the "Cobalt Group" by Parks and Swartley (1916). Ramp (1964) reported that ore samples contained 0.2 weight percent Cu and traces of Ni, Au, and Co.

SULFIDE OCCURRENCE

Pods and stringers of sulfide are exposed in the cliffs along the Illinois River in an area where late, steeply dipping faults have juxtaposed medium-grained, massive, and relatively undeformed pyroxene cumulates against a sequence of deformed and mineralogically and texturally diverse rocks that are predominantly gabbroic (fig. 2).

Both rock types contain distinctive sulfide assemblages. Most abundant are pyrrhotite-rich massive pods or disseminated sulfides that occur primarily in the pyroxene cumulates. The largest of the massive pods measures approximately 10 m by 5 m and has been explored to a tunneled depth of 15 m. Locally, these sulfides have been remobilized during faulting and are now stringers in the fault that separates the pyroxenite from metagabbroic rocks (fig. 2). Where injected along this fault, the sulfides are found within both rock types.

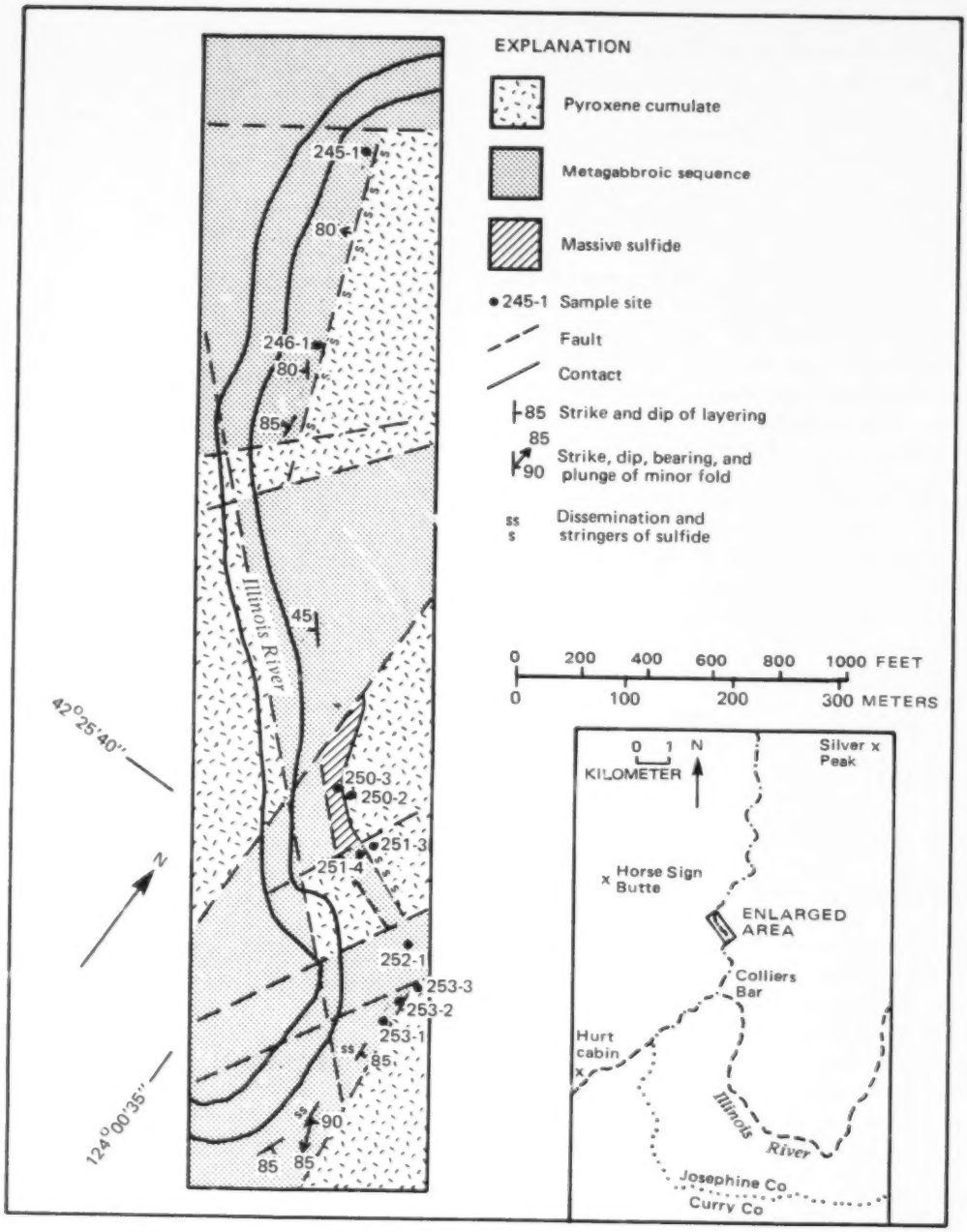

Figure 2. Geology of the Illinois River sulfide occurrence. Sample locations shown by dots.

The second class of sulfides are rare pyrite-rich stringers that occur only in the metagabbroic rocks. These are thin (less than 0.3 m) and discontinuous (less than 3 m in length) layers that conform to the layering of the surrounding rocks. Their sporadic distribution apparently was not controlled either by proximity to pyroxenite or by the presence of faults and shears.

LITHOLOGY

Pyroxene Cumulates

The pyroxene cumulates are massive, unlayered, and medium grained. Except where gossans are present, exposures are dark gray to black. Blocky clinopyroxene is the most abundant and in the field is usually the only

recognizable mineral; good cumulus textures are observed where small amounts of interstitial plagioclase or disseminated sulfides are present. The pyroxenites do not have a recognizable igneous lamination or a secondary foliation. Representative modes are given in table 1.

In rocks that are almost monomineralic, clinopyroxene forms 3–6-mm grains that have a xenomorphic granular texture. Most grains have a subhedral core, 1 to 2 mm wide, that contains orthopyroxene exsolution and is surrounded by an anhedral, exsolution-free rim. In rocks less rich in clinopyroxene, grains are more typically subhedral, 1 to 3 mm in size, and contain uniformly distributed orthopyroxene inclusions. In many places, clinopyroxenes have growth twins; although some show slight undulatory extinction, kink bands and deformation lamellae are uncommon.

Olivine, orthopyroxene, and plagioclase are relatively rare and are the only other primary silicates. Olivine occurs both as a cumulus phase and as adcumulus interstitial masses. Cumulus euhedral olivine, 0.5 to 1 mm in size, is enclosed in plagioclase and orthopyroxene. Rarely, euhedral olivine is found within large euhedral clinopyroxene. Interstitial olivine occurs as anhedral masses and as stringers connected to euhedral olivine grains. Orthopyroxene occurs principally as anhedral reaction rims around euhedral olivine, but, in some samples, orthopyroxene (1–3 mm) has a euhedral form and may be enclosed by interstitial plagioclase or clinopyroxene. Plagioclase is always an interstitial phase between euhedral cumulus pyroxenes or olivine. Minor sericitic alteration is present in most places.

Serpentine and hornblende are alteration phases. Hornblende occurs mostly as isolated patches that have replaced clinopyroxene. Serpentine replaces olivine and pyroxene and forms bastite and mesh-textured masses, which X-ray examination shows to be lizardite. Serpentine is most pervasive where sulfides are abundant.

Disseminated to massive sulfide occurs within the pyroxenite. Most sulfides are disseminated cuspate masses found along the grain boundaries of euhedral pyroxene and olivine. Where more abundant, these sulfides have net textures that enclose euhedral silicate grains. Where massive, sulfides typically include isolated grains of euhedral clinopyroxene or olivine (fig. 3*A*). Less common are sulfide blebs which have a maximum diameter of 1 mm and which have been found in clinopyroxene and orthopyroxene, but not in olivine (fig. 3*B*, *C*).

Primary sulfide mineralogy is simple and uniform. Most sulfides (60–80 percent) are pyrrhotite, which X-ray diffraction, treatment with a magnetic colloid solution, and electron microprobe analysis show to be almost entirely hexagonal with very minor intergrowths of the monoclinic phase. Pyrrhotite occurs as small (<0.5 mm) blebs enclosed in silicates, as anhedral grains molded around silicates, or as masses that enclose euhedral silicates. Isolated grains commonly also contain chalcopyrite and pentlandite. Large masses of pyrrhotite, however, generally do not have other sulfide phases. Chalcopyrite makes up most of the remaining (15–30 percent) sulfides, either as blocky or lamellae-shaped exsolutions in pyrrhotite blebs or as stringers and anhedral masses within massive pyrrhotite. It is rarely found as isolated grains. Cubanite is present in trace amounts as exsolution lamellae in chalcopyrite. Pentlandite (less than 5 percent of the sulfide) always occurs in pyrrhotite. It is most abundant in small pyrrhotite blebs where it typically forms small (<0.3 mm) blocky grains near pyrrhotite-silicate boundaries. In massive pyrrhotite, pentlandite may form thin stringers or small disseminated grains that are entirely within pyrrhotite.

In pyroxenites, pyrite is found only in massive sulfide (samples 253–3 and 250–3) where it forms isolated 1–3-mm subhedral grains, birds-eye alterations on pyrrhotite, and less common stringers and lamellae enclosed in pyrrhotite.

Secondary magnetite and hematite are found in trace amounts in disseminated sulfides and are abundant in massive sulfides.

Silicate textures clearly show the rocks to be clinopyroxene, clinopyroxene-olivine, clinopyroxene-orthopyroxene, and clinopyroxene-orthopyroxene-olivine cumulates. Nearly monomineralic clinopyroxenites are good adcumulates. They show anhedral rims around subhedral clinopyroxene cores that contain abundant orthopyroxene exsolution lamellae. Most other rocks are mesocumulates showing both adcumulus growth and crystallization of trapped interstitial liquid. Although the layered sequence of diverse rock types needed to establish a crystallization trend is not present, cumulus parts of ophiolites typically start with the precipitation of olivine followed by olivine+clinopyroxene (Coleman, 1977). Plagioclase crystallization usually follows crystallization of olivine+clinopyroxene, although, in some places, minor amounts of orthopyroxene appear before plagioclase (Himmelberg and Loney, 1980). In these rocks, the inclusion of some euhedral olivine in cumulate clinopyroxenes suggests that olivine was locally the first phase to crystallize and that it was followed by clinopyroxene and minor amounts of orthopyroxene.

The mineralogy and textures of the sulfides in the pyroxenite are characteristic of magmatic sulfide deposits. The primary mineralogy of magmatic sulfides is usually very simple and consists dominantly of pyrrhotite with minor chalcopyrite and pentlandite. In this occurrence, these three phases are present in sulfide blebs that are enclosed within cumulus silicate grains; the textural relationship shows that an immiscible sulfide liquid existed while cumulus silicate minerals were crystallizing. This intergrowth of pyrrhotite, chalcopyrite, and pentlandite constitutes the expected exsolution product formed upon crystallization from typical magmatic Cu-Ni-Fe-S liquids (Kullerud and others, 1969; Craig and Scott, 1974). Additional textural evidence

Table 1. Modal compositions of rock units

[Sample locations given on figure 2; modes based on a minimum of 1,000 points per thin section]

	Pyroxene cumulate				Metagabbroic sequence					
Sample number	250–2	250–3	251–3	253–3	245–1	246–1	251–4	252–1	253–1	253–2
Clinopyroxene	56.14	40.30	61.70	19.53	15.81	16.95	-----	-----	-----	-----
Plagioclase	24.07	-----	-----	-----	36.58	39.74	4.30	21.49	-----	39.33
Orthopyroxene	1.62	-----	20.95	-----	5.77	8.66	28.71	-----	-----	30.83
Olivine	-----	1.61	3.02	-----	-----	-----	-----	-----	-----	-----
Serpentine	6.62	39.14	-----	46.99	-----	-----	.59	-----	-----	-----
Hornblende	6.65	-----	9.57	-----	25.77	33.12	-----	56.31	-----	-----
Cordierite	-----	-----	-----	-----	-----	-----	38.62	-----	-----	7.32
Quartz	-----	-----	-----	-----	6.09	-----	-----	14.20	48.59	-----
Epidote	-----	-----	-----	-----	-----	-----	-----	-----	29.34	4.64
Biotite	-----	-----	-----	-----	-----	-----	3.03	-----	-----	-----
Chlorite	-----	-----	-----	-----	-----	-----	-----	-----	17.05	-----
Sulfides	4.90	18.95	4.76	21.56	3.00	1.53	24.75	6.68	5.02	14.36
Oxides	tr	tr	tr	11.92	6.98	tr	tr	1.32	tr	3.52

of magmatic sulfide accumulation consists of the euhedral silicates disseminated within massive sulfide and the interconnected, cuspate sulfides in net-textured sulfides (Naldrett, 1973, 1979).

Metagabbroic Sequence

Metamorphosed and deformed rocks of predominantly gabbroic compositions are in fault contact with the pyroxenites and are referred to here as the metagabbroic sequence. Most are fine- to medium-grained dark-gray rocks that range from rare epidote-chlorite-quartz gneiss to more common interlayered sequences of clinopyroxene-orthopyroxene-plagioclase-hornblende ± quartz, cordierite-plagioclase-orthopyroxene ± quartz, and quartz-plagioclase-hornblende gneisses. The rocks are commonly finely layered to massive and are well foliated. The foliation parallels axial surfaces of tight to isoclinal minor folds and crosscuts compositional layering in fold noses. Rare concordant sulfide stringers are present within some gneisses and are also folded and cut by axial planar foliations.

With the exception of hornblende, most minerals are smaller than 1 mm and form anhedral masses that have strong undulatory extinctions. Textures are mostly blastomylonitic, although locally porphyroclasts of clinopyroxenes and pyrite occur. Mineral phases are described briefly below, and modes of metagabbroic rocks are given in table 1.

Blue-green and green-brown amphiboles occur as alteration around clinopyroxene and orthopyroxene and as subhedral laths as long as 3 mm. Laths lie in and, in many places, conspicuously define the foliation. Many large hornblendes are spongelike masses that enclose all other mineral phases in the rock. Modal variation in hornblende forms the most recognizable compositional layering.

Small anhedral grains of both clinopyroxene (1.0 mm) and orthopyroxene (0.5 mm) occur as untwinned, anhedral grains that show slight undulatory extinction and are aligned in the foliation. In blastomylonitic rocks (sample 246–1), some clinopyroxene also makes twinned (3 mm) porphyroblasts. In contrast, orthopyroxene may occur as large (2 to 3 mm) unstrained spongelike masses that enclose all other minerals except hornblende.

Anhedral quartz that has strong undulatory extinction, cordierite that appears similar to quartz, and slightly sericitized anhedral and twinned plagioclase commonly occur as grains as large as 1 mm. Larger grains of quartz (to 3 mm) are formed in the epidote-chlorite-quartz gneiss (sample 253–1) and are rimmed by masses of chlorite.

Minor secondary anhedral epidote (<1 mm), occurring with chlorite and biotite that alter both pyroxene and hornblende, is locally present.

Sulfides in the metagabbroic rocks are dominantly pyrite and also contain lesser amounts of chalcopyrite and scarce pyrrhotite. Anhedral grains (<0.5 mm) and rare granulated subhedral cubes (to 1 mm) of pyrite typically constitute between 50 to 90 percent of the sulfides. Chalcopyrite constitutes between 5 to 15 percent of the sulfides and occurs as rims around pyrite and as small replacements patches in pyrite. Pyrrhotite is rare except where faults have placed rocks near pyrrhotite-rich pods hosted in pyroxene cumulates (sample 251–4). In these pods, pyrrhotite, which appears to have been mobilized from the adjacent cumulates, may constitute more than 80 percent of the sulfide. More typically, pyrrhotite makes up less than 5 percent of the sulfides and occurs as small (<0.3 mm) grains and embaying alterations on pyrite. Locally, small pyrite cubes

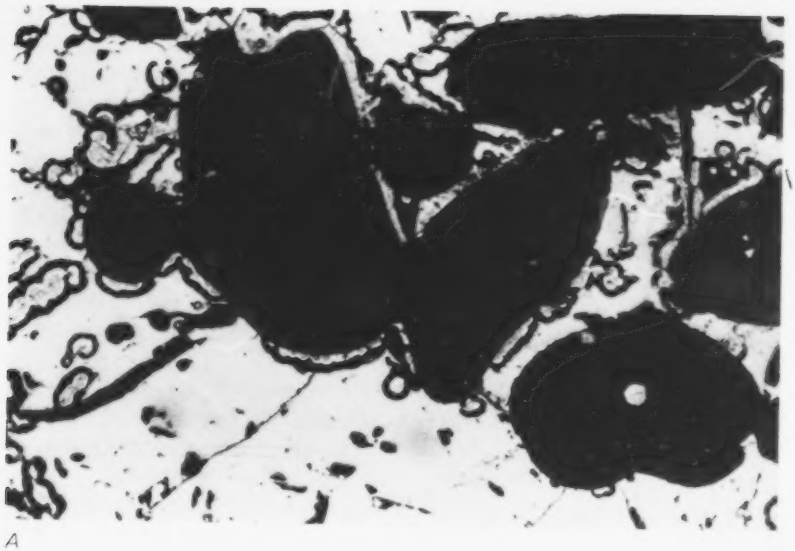

A

B

C

Figure 3. Photomicrographs of sulfides in pyroxenite. *A*, Reflected light showing subhedral clinopyroxenes enclosed in massive sulfide. Note small sulfide bleb included in lower-right clinopyroxene. *B*, Cumulus orthopyroxene enclosing two sulfide blebs and enclosed by lighter gray intercumulus plagioclase in transmitted light. *C*, Upper sulfide bleb from *B* shown in reflected light. Po-pyrrhotite, Cp-chalcopyrite, Pt-pentlandite. Approximate long dimensions of photographs are 4 mm for *A* and *B*, 2 mm for *C*.

have been completely replaced by pyrrhotite. Pentlandite has not been found in the metagabbroic units.

Patchy secondary magnetite and hematite are associated mostly with sulfides. However, compositional layering in some rocks (sample 245–1) is partly outlined by disseminated layers of subhedral magnetite grains that are smaller than 0.5 mm.

Megascopic and microscopic examinations show that the metagabbroic rocks have been highly deformed and metamorphosed. The tight to isoclinal folds and the penetrative mineral foliation are the result of at least one intense deformation. Also, the occurrence of orthopyroxene as both small strained grains and as large, unstrained and poikilliticaly enclosing masses indicates that granulite-grade metamorphism took place both during and after deformation (Winkler, 1967). Other evidence for granulite-grade metamorphism is from pyroxene geothermometry (discussed below) that indicates metamorphic temperatures of approximately 900°C. The pressure of metamorphism is less well defined. The presence of cordierite without garnet has traditionally been interpreted as a low-pressure assemblage that would place these rocks in the low-pressure subfacies of the granulite facies as defined by Miyashiro (1973). However, the reaction that produces garnet from cordierite as pressure increases also is dependent on Mg/(Mg+Fe). Studies by Henson and Green (1972) of systems without excess aluminum show that cordierite compositions with Mg/(Mg+Fe)=0.9 (similar to those in this unit), which are in the assemblage cordierite-hypersthene-quartz, may be stable to a maximum of 8–9 kilobars. Metamorphism may therefore have taken place at depths as great as 30 km.

The metagabbroic sequence can be directly correlated with rocks of similar composition that make up the Big Craggies to the south. These rocks have also been deformed by at least one penetrative deformation and metamorphosed to granulite grade (Coleman, 1972; Ramp, 1975). Furthermore, these rocks are also similar to sheared gabbroic rocks which make up parts of the adjacent Chetco River complex and which have been interpreted as part of an island-arc complex (Nicholson, 1981). Regardless of environment of formation, the deformation, metamorphism, and type of mineralization shown by this unit are in sharp contrast to the pyrrhotite-rich mineralization found in the adjacent pyroxenite, and they lead to the conclusion that relatively recent and steeply dipping faults have juxtaposed part of a highly deformed and metamorphosed gabbroic complex with minor stringers of pyrite-chalcopyrite mineralization against a fragment of oceanic crust containing magmatic pyrrhotite-chalcopyrite-pentlandite mineralization.

MINERAL AND ROCK ANALYSES

Mineral compositions were determined for all primary phases and for some secondary hornblendes in the pyroxenite. Compositions were obtained by means of an ARL–EMX SM microprobe in which combined wave-length and energy-dispersive systems were used. Operating conditions were 15 kV and 0.1 microamp beam current. In analyses of silicates, natural and synthetic standards and matrix corrections were used, and the procedures of Bence and Albee (1968) and Albee and Ray (1970) were followed. In analyses of sulfides, synthetic standards and data were reduced by means of the ZAF computer program provided by Tracor Northern.[1] Analytical results and structural formulas are given in tables 2–8. All compositions are averages from at least three grains, on which at least two spots were analyzed.

Pyroxenes (table 2, 3; fig. 4) from the pyroxenite are richer in Mg and are more uniform in composition than those from the metagabbroic sequence. As previously described, some grains have exsolution-rich cores and exsolution-free rims. Analyses made between visible exsolution lamellae in grain centers are similar to analyses obtained on exsolution-free grain rims. No compositional differences were found between cumulate and intercumulate grains in the pyroxenite or between pre- and post-deformation grains in the metagabbroic rocks. Pyroxenes from the pyroxenite have uniform and low Al_2O_3 (<2 weight percent); orthopyroxenes from the metagabbro have somewhat higher Al_2O_3 and MnO contents than those from the pyroxenite.

Olivines (table 4) are Fo_{79-87}. Nickel contents are less than 0.07 percent, which is lower than values typically found in magmatic olivines of this composition (Simkin and Smith, 1970). However, Duke and Naldrett (1978) and Duke (1979) showed that similar low-nickel contents can result when olivine is crystallized from a melt that is already saturated with, and is precipitating, immiscible sulfides.

Plagioclase (table 5) is rarely found in the pyroxenite as intercumulus grains of composition An_{87}. Within the metagabbro, plagioclase ranges from An_{46} to An_{88}, and no apparent correlation exists between rock mineralogy and plagioclase composition.

Amphiboles (table 6) were chemically characterized by means of the method of Papike and others (1974). Analyses of two amphiboles occurring as brown alteration patches of magnesiokaersutite in pyroxenite show widely variable amounts of other than quadrilateral components. In contrast, the primary amphiboles from the metagabbroic sequence are more compositionally uniform magnesiokaersutites, containing 62 to 65 percent other than quadrilateral components.

Cordierite (table 7) is Mg rich (Mg/(Mg+Fe)=86 to 91). Totals of analyses are slightly less than 100, which suggest that some structural water might be present.

[1]Any trade names in this publication are used for descriptive purposes only and do not constitute endorsements by the U.S. Geological Survey.

Table 2. Electron microprobe analyses of clinopyroxene
[Standard deviations in parentheses]

Sample number	Pyroxene cumulate				Metagabbroic sequence	
	250–2	250–3	251–3	253–3	245–1	246–1
Weight percent						
SiO_2	53.6	52.9	52.6	53.5	52.6	52.6
	(.574)	(.346)	(.159)	(.076)	(.923)	(.784)
Al_2O_3	.48	1.80	1.10	1.21	1.50	.50
	(.091)	(.092)	(.019)	(.063)	(.156)	(.191)
[1]FeO	5.02	3.96	5.30	4.33	9.22	7.21
	(.108)	(.141)	(.269)	(.226)	(.256)	(1.02)
MnO	.16	.31	.19	---	.50	.25
	(.028)	(.155)	(.164)	(.130)	(.098)	(.042)
MgO	16.9	16.7	16.6	16.8	14.2	15.3
	(.409)	(.601)	(.343)	(.305)	(.316)	(.049)
CaO	23.4	23.6	22.9	23.7	21.2	22.5
	(.633)	(.177)	(.411)	(.209)	(.348)	(.530)
Na_2O	---	.32	.21	.11	.22	.10
	(.000)	(.169)	(.030)	(.168)	(.035)	(.141)
TiO_2	.20	.17	.03	.08	.14	.27
	(.048)	(.007)	(.000)	(.047)	(.080)	(.261)
Cr_2O_3	.27	.26	.17	.31	.03	.01
	(.051)	(.021)	(.083)	(.127)	(.011)	(.021)
NiO	.05	.02	.01	.05	.02	.02
	(.037)	(.014)	(.015)	(.023)	(.021)	(.028)
Total	100.08	100.04	99.11	100.09	99.63	98.76
Cations per 6 oxygens						
Si	1.970	1.940	1.954	1.960	1.967	1.976
Al^{IV}	.021	.060	.046	.040	.033	.022
Sum TET	1.991	2.000	2.000	2.000	2.000	1.998
Al^{VI}	.000	.018	.002	.012	.033	---
Fe^{+2}	.154	.121	.165	.133	.288	.227
Mn	.005	.010	.006	.000	.016	.008
Mg	.923	.913	.920	.917	.793	.855
Ca	.922	.926	.911	.929	.851	.905
Na	.000	.023	.015	.008	.016	.007
Ti	.006	.005	.001	.002	.004	.008
Cr	.008	.008	.005	.009	.001	.000
Ni	.001	.001	.000	.001	.001	.001
Sum OCT	2.019	2.025	2.025	2.011	2.003	2.011
$\frac{100 \times Mg}{Mg+Fe+Mn}$	85.3	87.5	84.3	87.3	72.30	78.4
En	46.2	46.6	46.1	46.4	41.1	43.0
Fs	7.7	6.2	8.3	6.7	14.9	11.5
Wo	46.1	47.2	45.6	46.9	44.0	45.5

[1]Total Fe as FeO.

Table 3. Electron microprobe analyses of orthopyroxene
[Standard deviations in parentheses]

Sample number	Pyroxene cumulate		Metagabbroic sequence			
	250–2	251–3	245–1	246–1	251–4	253–2
Weight percent						
SiO_2	56.3	55.5	51.6	55.00	53.5	53.0
	(.396)	(.260)	(.858)	(.088)	(.431)	(.515)
Al_2O_3	.01	.49	1.03	—	2.17	2.91
	(.042)	(.002)	(.023)	(.000)	(.148)	(.149)
[1]FeO	12.5	12.0	24.9	15.7	14.1	20.4
	(.357)	(.299)	(.096)	(.530)	(.064)	(.212)
MnO	.33	.34	.76	.55	.40	.94
	(.059)	(.124)	(.152)	(.068)	(.035)	(.096)
MgO	29.5	29.5	19.5	27.0	28.8	23.9
	(.259)	(.054)	(.286)	(.325)	(.092)	(.631)
CaO	1.26	1.40	.82	.67	.18	.20
	(.053)	(.573)	(.023)	(.187)	(.099)	(.030)
Na_2O	—	—	—	.08	.09	—
	(.000)	(.000)	(.000)	(.090)	(.001)	(.000)
TiO_2	.04	.05	.02	.11	.03	.08
	(.053)	(.058)	(.075)	(.055)	(.035)	(.056)
Cr_2O_3	.13	.06	—	.02	—	.08
	(.051)	(.054)	(.000)	(.026)	(.000)	(.040)
NiO	.06	.04	.03	—	.01	.06
	(.020)	(.030)	(.001)	(.028)	(.049)	(.011)
Total	100.13	99.38	98.66	99.13	99.28	101.57
Cations per 6 oxygens						
Si	1.999	1.984	1.979	2.002	1.930	1.926
Al^{IV}	.000	.016	.021	.000	.070	.074
Sum TET	1.999	2.000	2.000	2.002	2.000	2.000
Al^{VI}	.000	.005	.026	.000	.022	.051
Fe^{+2}	.370	.360	.798	.479	.427	.620
Mn	.010	.010	.025	.017	.012	.029
Mg	1.565	1.570	1.113	1.465	1.550	1.294
Ca	.048	.054	.034	.026	.007	.008
Na	.000	.000	.000	.006	.006	.000
Ti	.001	.001	.001	.003	.001	.002
Cr	.004	.002	.000	.001	.000	.002
Ni	.002	.001	.001	.000	.000	.002
Sum OCT	2.000	2.003	1.998	1.997	2.025	2.008
$\frac{100 \times Mg}{Mg+Fe+Mn}$	80.5	80.9	57.5	74.7	77.9	66.6
En	78.9	79.1	57.2	74.4	78.1	67.3
Fs	18.7	18.2	41.0	24.3	21.5	32.3
Wo	2.4	2.7	1.8	1.3	0.4	0.4

[1]Total Fe as FeO.

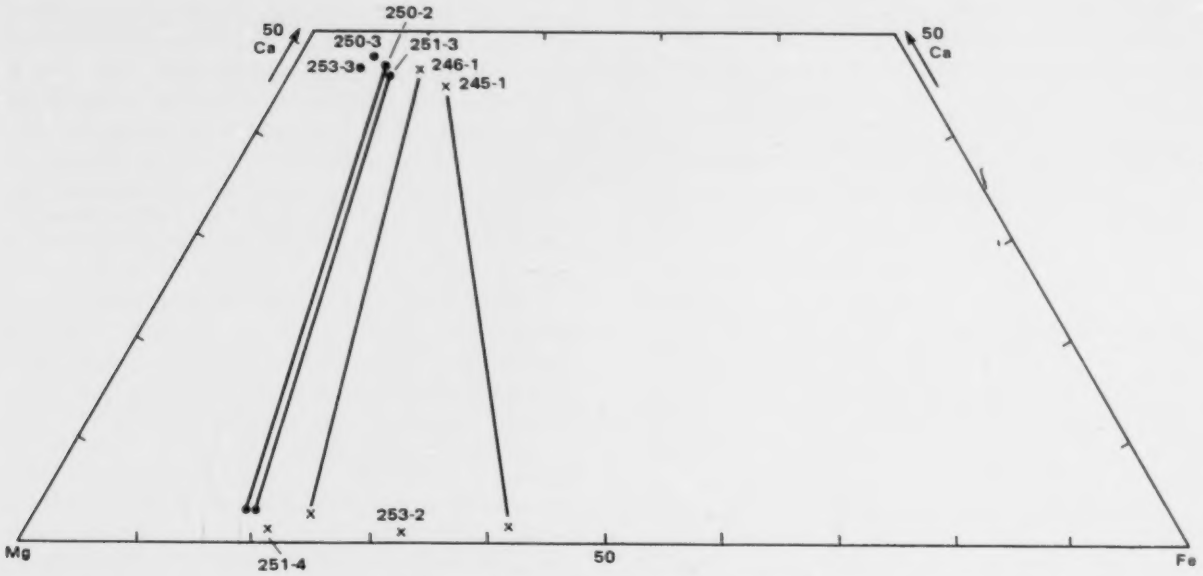

Figure 4. Plot of pyroxene compositions in the Ca-Mg-Fe ternary (atomic percent). Dots–cumulus pyroxenite; crosses–metagabbroic sequence.

Compositions of cumulus pyroxenes and olivines as well as intercumulus plagioclase in the pyroxenite are similar to those reported from cumulus zones in other ophiolite complexes (for example, Coleman, 1977; Himmelberg and Loney, 1980; England and Davies, 1973; Jackson and others, 1975; Juteau and Whitechurch, 1980). They are also similar to Gray's (1980) description of ultramafic rocks near Tincup Peak in the Chetco River complex, southeast of this study area (fig. 1). Silicates from the metagabbroic sequence are chemically more diverse. Pyroxene, plagioclase, and amphibole in much of this sequence have compositions similar to those found in sheared gabbroic rocks of the adjacent Chetco River complex, which has been interpreted as part of a volcanic-arc sequence (Nicholson, 1981).

Sulfides (compositions in tables 8–11) may be divided into those within pyroxenite and those within the metagabbroic rocks.

The sulfides in pyroxenite are either disseminated blebs (samples 250–2 and 251–3) or massive and interconnected concentrations (samples 250–3 and 253–3). The blebs are interpreted to be frozen immiscible droplets, and their compositions probably most closely approximate unaltered values. The more massive concentrations appear to be sulfides remobilized adjacent to faults and to have altered compositions. Pentlandites (table 8) from the droplets contain nearly 6 weight percent cobalt. This is significantly higher than the 0 to 2 weight percent cobalt found in most magmatic pentlandites that are associated with pyrrhotite, but it is within the range recorded from some sulfide deposits (Harris and Nickel, 1972). Adjusting these pentlandite compositions by adding proportional amounts of the metals present as cobalt to iron and nickel results in compositions that have "adjusted" nickel contents, which, with the exception of the most cobalt-rich pentlandite (sample 250–3), are similar to those observed in other low-cobalt or "adjusted" natural pentlandites that occur with pyrrhotite (Misra and Fleet, 1973). In contrast, pentlandites in samples containing interconnected sulfides (250–3 and 253–3) have widely different and remarkably high cobalt contents (21 to 36 weight percent). Pentlandites containing similar amounts of cobalt have been reported from a few other environments, among which are the copper ores hosted in quartzites at Outokupu, Finland (Kouvo and others, 1959; Huhma, 1970), ores at Cobalt, Ontario, Canada (Petruk and others, 1969), and ores in serpentinized wehrlites in Japan (Matsuhara and Kato, 1979). Although the means by which these pentlandites formed are not always clear, a variety of nonmagmatic processes seem to have been involved. The high cobalt content of the pentlandites in samples 250–3 and 253–3 thus indicates that compositions of these sulfides have been altered, a conclusion compatible with the field relationships, which show the sulfides to have been mobilized within faults and shears.

Pyrrhotites (table 9) in these interconnected sulfides have cobalt and nickel contents (0.3–0.4 weight percent Co and 0.2–0.4 weight percent Ni) that are respectively higher and lower than in the disseminated sulfides (0.0–0.07 weight percent Co; 0.41–0.53 weight percent Ni). Chalcopyrites (table 10) in both types of sulfides are similar in composition. Pyrite (table 11) occurs in the massive sulfides; one sample contains almost 1 weight percent Ni.

Table 4. Electron microprobe analyses of olivine
[Standard deviations in parentheses]

	Pyroxene cumulate	
Sample number ---	250–3	251–3
Weight percent		
SiO_2 ----------	40.3	40.3
	(.215)	(.336)
[1]FeO ----------	12.9	18.6
	(.281)	(.245)
MnO ----------	.18	.21
	(0.28)	(.108)
MgO ----------	46.3	41.2
	(.953)	(.669)
CaO ----------	.13	.16
	(.056)	(.045)
NiO ----------	.03	.07
	(.029)	(.041)
Cr_2O_3 ----------	.05	.00
	(.075)	(.000)
Total ---------	99.89	100.54
Cations per 4 oxygens		
Si ----------	1.002	1.021
Fe ----------	.269	.394
Mn ----------	.004	.005
Mg ----------	1.717	1.553
Ca ----------	.003	.004
Ni ----------	.001	.001
Cr ----------	.001	.000
Sum cations ---	2.997	2.978
$\frac{100 \times Mg}{Mg+Fe+Mn}$	86.3	79.6

[1]Total Fe as FeO.

Sulfides within the metagabbro are mostly stringers and disseminations of compositionally similar pyrites and chalcopyrite. Near faults, pyrite is locally replaced by minor amounts of pyrrhotite that has nickel (0.13 percent) and cobalt (0.06 percent) contents similar to amounts found in the host pyrite. In faults, the metagabbro locally also has massive pods of pyrrhotite (sample 251–4) that is similar in composition to the pyrrhotite in the adjacent pyroxenite (0.3 percent nickel; 0.1 percent cobalt).

Five whole-rock analyses of samples, which were either from disseminated sulfides in pyroxenite or from interconnected sulfides in faults or shears in pyroxenite or in the metagabbroic sequence, were obtained for Ni, Cu, Co, S, Pt, Pd, Rh, and Au. Metal values are given in table 12, and the analyses recalculated to 100 percent sulfides are shown in table 13. Recalculation to 100 percent sulfide is necessary to minimize effects of differing proportions of sulfides to silicates and allows comparison of the sulfide composition from a wide variety of deposits. Mineral compositions (tables 8–11) were used in calculations for table 13. Norms calculated from table 13 approximate observed abundances. In addition, the recalculated noble-metal data have been normalized with respect to average chondritic meteorites (fig. 5) in the manner presented by Naldrett and others (1979).

The highest nickel, copper, and noble-metal concentrations in 100 percent sulfides are in samples containing disseminated sulfides (250–2, 251–3) that probably most closely approximate magmatic sulfide liquid compositions. In comparison, interconnected sulfides in pyroxenite (250–3, 253–3) and in metagabbro (251–4) show much lower amounts of Cu, Ni, platinum group metals (PGM's), and Au, and slightly higher concentrations of Fe and S. These concentrations suggest three possibilities: iron and sulfur have been added, the other elements have been depleted during fault-related mobilization, or an initially irregular distribution of metals existed. The second possibility is considered unlikely because such large primary changes in metal content over such short distances are unlikely and also because the interconnected sulfides hosted in pyroxenite (250–3 and 253–3) are geochemically similar to those occurring along faults that are entirely within metagabbroic rocks (251–4). Furthermore, the variations in metal-metal and metal-sulfur ratios between disseminated and interconnected sulfides (table 14) are consistent with differential loss of metals due to differing geochemical behavior of elements during mobilization; this suggests that the interconnected sulfides did not form by dilution resulting from the addition of Fe and S. The nearly constant Fe/S, but slight decrease in (Fe+Ni+Cu+Co)/S, suggests that formation of interconnected sulfides involved removal of Cu, Ni, and Co; the relatively small decrease in Ni/Cu and larger decrease in Ni/Co shows Ni to be slightly more depleted than Cu and much more depleted than Co in the interconnected sulfides. This relative enrichment of Co relative to Ni and Cu is consistent with the extremely cobalt-rich pentlandites observed in the interconnected sulfides. Relative concentrations of precious metals appear unchanged between the interconnected and disseminated sulfides.

The compositions of 100 percent sulfides in pyroxenite have been plotted on the Fe-Ni-S ternary diagram (fig. 6). In this diagram, the sulfide compositions were corrected by removing the metals and sulfur present in chalcopyrite and by adding proportional amounts of cobalt present to iron and nickel. With the exception of sample 253–3, all samples fall in the monosulfide solid-solution ($(Fe,Ni)_{1-x}S$ or Mss) field at 500°C (Naldrett and others, 1967); this indicates that exsolution occurred below this temperature to yield the observed sulfide phases. Samples 250–2 and 251–3, which

Table 5. Electron microprobe analyses of plagioclase
[Standard deviations in parentheses]

Sample number	Pyroxene cumulate	Metagabbroic sequence				
	250–2	245–1	246–1	251–4	252–1	253–2
Weight percent						
SiO_2	47.0	52.8	46.7	47.3	56.4	55.6
	(.876)	(.956)	(.452)	(.812)	(.015)	(.505)
Al_2O_3	34.0	30.9	35.4	34.5	27.7	28.4
	(.532)	(.870)	(.337)	(.054)	(.753)	(.492)
[1]FeO	.02	.24	.55	.24	.08	.25
	(.074)	(.092)	(.126)	(.078)	(.001)	(.161)
CaO	17.7	12.8	17.7	16.9	9.6	10.3
	(.325)	(.436)	(.233)	(.389)	(.005)	(.304)
Na_2O	1.22	4.20	1.12	1.39	6.03	5.88
	(.224)	(.199)	(.556)	(.355)	(.152)	(.148)
K_2O	.28	.00	.30	.25	.13	.17
	(.014)	(.000)	(.263)	(.052)	(.151)	(.061)
Total	100.22	100.94	101.77	100.58	99.94	100.60
Cations per 32 oxygens						
Si	8.625	9.474	8.460	8.626	10.126	9.971
Al	7.352	6.548	7.554	7.417	5.876	5.995
Fe	.003	.036	.083	.037	.012	.037
Ca	3.469	2.464	3.434	3.312	1.858	1.987
Na	.433	1.462	.394	.492	2.101	2.045
K	.065	.000	.069	.058	.030	.039
Sum cations	19.947	19.984	19.994	19.942	20.003	20.074
End member proportions						
Or	1.6	0.0	1.8	1.5	0.7	1.0
Ab	10.9	37.2	10.1	12.7	52.7	50.2
An	87.5	62.8	88.1	85.8	46.6	48.8

[1]Total Fe as FeO.

may more closely reflect actual magmatic sulfide compositions, plot near the center of the Mss field and would probably not exsolve pentlandite until temperatures dropped below 300°C. The copper content of these disseminated sulfides is between 7 and 12 weight percent, which would exceed the solubility of chalcopyrite in Mss below 500°C (Kullerud and otners, 1969) and which indicates that an intermediate solid solution (Cu-Fe-S solid solution or Iss) must have been present.

Although the sulfides were hosted in a clinopyroxenite cumulate, three chemical features suggest that the sulfides formed in equilibrium with gabbroic liquids. Naldrett and Cabri (1976) established relationships between Ni/Cu and magma composition showing that Ni/Cu of 0.19 to 0.21, such as found in samples 250–2 and 251–3, would be in equilibrium with gabbroic liquids that contain less than 10 weight percent MgO. Naldrett and Cabri (1976) also determined that Pt/Pd in sulfides precipitating from nonkomatiitic liquids decrease as Ni/Cu decreases such that the Pt/Pd values of 0.30 and 0.49, observed in samples 250–2 and 251–3, are also expected values from liquids containing about 10 weight percent MgO. Finally, the work of Naldrett and others (1979) and Naldrett (1981) established that chondrite normalized patterns for PGM's and Au in sulfides from gabbro-hosted nickel deposits have a sloping trend that is distinctly different from the flatter pattern made by sulfides precipitated from ultramafic (komatiitic) liquids. The steep increase from Rh to Au in the Illinois River sulfides (fig. 5) is comparable with the sloping pattern made by the gabbro-hosted Sudbury ores.

Table 6. Electron microprobe analyses of amphibole
[Standard deviations in parentheses]

	Pyroxene cumulate		Metagabbroic sequence		
Sample number	250–2	251–3	245–1	246–1	252–1
		Weight percent			
SiO_2	52.0	48.3	46.6	46.4	47.2
	(.272)	(.135)	(.406)	(.487)	(.856)
Al_2O_3	5.73	7.67	9.15	11.7	11.6
	(.171)	(.197)	(.078)	(1.03)	(.202)
[1]FeO	6.54	7.72	14.2	10.93	11.5
	(.110)	(.172)	(.127)	(.106)	(.628)
MnO	.21	.11	.18	.10	.31
	(.035)	(.054)	(.002)	(.162)	(.215)
MgO	18.4	17.4	12.7	15.1	14.0
	(.119)	(.253)	(.106)	(.339)	(.480)
CaO	13.1	12.4	11.8	12.6	11.6
	(.022)	(.158)	(.290)	(.028)	(.550)
Na_2O	.66	1.21	1.33	1.73	1.10
	(.126)	(.029)	(.106)	(.021)	(.033)
K_2O	.52	.79	.17	.13	.13
	(.111)	(.077)	(.106)	(.110)	(.050)
TiO_2	1.08	1.49	1.39	.74	.92
	(.171)	(.109)	(.148)	(.028)	(.212)
Cr_2O_3	.64	.32	—	.14	.00
	(.032)	(.044)	(.007)	(.077)	(.000)
Total	98.88	97.41	97.52	99.57	98.36
Fe_2O_3	.05	1.61	2.28	3.98	3.66
FeO	6.50	6.27	12.2	7.35	8.23
New Total	98.89	97.57	97.80	99.97	98.75
		Cations			
Si	7.304	6.925	6.816	6.533	6.697
Al^{IV}	.696	1.075	1.184	1.467	1.303
Sum TET	8.000	8.000	8.000	8.000	8.000
Ti	.114	.161	.153	.078	.098
Al^{VI}	.252	.223	.393	.486	.637
Fe^{+3}	.005	.174	.251	.422	.391
Fe^{+2}	.762	.753	1.488	.867	.977
Mn	.025	.013	.022	.012	.037
Mg	3.843	3.720	2.764	3.176	2.967
Ca	1.967	1.907	1.842	1.912	1.768
Na	.180	.312	.377	.473	.303
K	.093	.145	.032	.023	.023
Sum Cations	15.241	15.408	15.322	15.449	15.201
[2]Quadrilateral components	65.21	46.25	40.81	26.66	34.85
[2]Ca	29.93	29.89	30.22	32.11	30.96
[2]Mg	58.47	58.31	45.36	53.34	51.94
[2]Fe^{+2}	11.60	11.80	24.41	14.55	17.10
[2]A	24.93	26.55	20.20	22.88	12.40
[2]NAM4	3.23	3.25	5.46	2.39	7.62
[2]AL4	71.84	70.20	74.34	74.72	79.98

[1]Total Fe as FeO.
[2]Definition and method of calculation given by Papike and others (1974).

Table 7. Electron microprobe analyses of cordierite
[Standard deviations in parentheses]

Sample number	Metagabbroic sequence	
	251–4	253–2
Weight percent		
SiO_2	48.9	48.7
	(.422)	(.621)
Al_2O_3	35.2	34.4
	(.381)	(.226)
[1]FeO	2.24	3.37
	(.005)	(.080)
MnO	.05	.02
	(.114)	(.020)
MgO	12.6	11.6
	(.085)	(.082)
CaO	---	.06
	(.000)	(.081)
Na_2O	.12	.18
	(.008)	(.008)
K_2O	---	---
	(.000)	(.000)
TiO_2	---	.00
	(.000)	(.000)
Total	99.11	98.33
Cations per 18 oxygen		
Si	4.866	4.906
Al	4.129	4.090
Fe	.186	.284
Mn	.004	.002
Mg	1.872	1.744
Ca	.000	.006
Na	.023	.035
K	.000	.000
Ti	.000	.000
Sum	11.080	11.067
Mg/Mg+Fe	.909	.860

[1]Total Fe as FeO.

Table 8. Electron microprobe analyses of pentlandite
[Wt, weight percent; At, atomic percent; SD, standard deviation. All analyses are averages of several points on several grains]

Sample number	Pyroxene cumulate			
	250–2	250–3	251–3	253–3
Fe—				
Wt	28.5	17.0	29.1	22.2
At	23.4	13.84	23.92	17.83
SD	(.461)	(.351)	(.642)	(.629)
Ni—				
Wt	33.2	13.9	31.5	24.0
At	25.87	10.73	24.55	18.33
SD	(.654)	(1.32)	(.502)	(.431)
Cu—				
Wt	.31	---	.50	---
At	.23	---	.36	---
SD	(.465)	---	(.283)	---
Co—				
Wt	5.71	36.0	5.39	21.5
At	4.44	27.76	4.19	16.37
SD	(.138)	(1.06)	(.421)	(.120)
S—				
Wt	32.2	33.7	32.9	34.0
At	46.06	47.07	46.99	47.47
SD	(.181)	(.747)	(.536)	(.742)
Total (Wt)	99.92	100.6	99.39	101.70
Metal/S	1.171	1.097	1.128	1.107

GEOTHERMOMETRY AND METAMORPHISM

Coexisting pyroxenes from four samples were used to estimate temperatures by means of the pyroxene geothermometer of Wells (1977). Samples 250–2 and 251–3 from cumulus pyroxenite respectively yield temperatures of 919°C and 923°C. Temperatures calculated from samples 245–1 and 246–1 from the metagabbroic sequence are 951°C and 897°C.

Bohlen and Essene (1979) reviewed the use of the two-pyroxene thermometer in metamorphic granulites and showed that experimental, analytical, and theoretical uncertainties cause the geothermometer to yield only approximate temperature data. Henry and Medaris (1980) recently evaluated the use of pyroxene geothermometers in southwest Oregon peridotites. They determined that each method has inherent differences that result in different temperatures. However, for pyroxenes equilibrated at relatively low temperatures (<1,000°C) and containing little Al_2O_3 (such as those studied here), the geothermometer proposed by Wells (1977) was believed to be the most reliable.

Temperatures obtained from peridotites adjacent to the Illinois River sulfide occurrence show that recrystallization took place over a temperature range of 1,200°C to 800°C (Henry and Medaris, 1980). Pyroxene augens yield temperatures between 1,200°C and 1,000°C, whereas matrix pyroxenes give lower temperatures between 1,000°C and 800°C. Himmelberg and Loney (1980) obtained temperatures between 975°C and 880°C from harzburgite, metacumulates, and cumulates within the Canyon Mountain Complex, Oregon, using Wells' geothermometer. The pyroxene cumulates at the Illinois River sulfide occurrence thus yield

Table 9. Electron microprobe analyses of pyrrhotite
[Wt, weight percent; At, atomic percent; SD, standard deviation]

	Pyroxene cumulate				Metagabbroic sequence	
Sample number ------	250–2	250–3	251–3	253–3	251–4	253–2
Fe—						
Wt ----------	60.0	60.3	60.9	59.6	60.4	60.6
At ----------	47.18	46.84	47.52	46.61	47.00	47.08
SD ----------	(.228)	(.550)	(.479)	(.954)	(.401)	(.242)
Ni—						
Wt ----------	.53	.24	.41	.41	.28	.13
At ----------	.39	.17	.31	.30	.22	.09
SD ----------	(.089)	(.180)	(.376)	(.180)	(.440)	(.100)
Cu—						
Wt ----------	.00	.12	.00	.24	.00	.05
At ----------	.00	.09	.00	.17	.00	.04
SD ----------	(.000)	(.167)	(.044)	(.191)	(.000)	(.095)
Co—						
Wt ----------	.00	.33	.07	.39	.11	.06
At ----------	.00	.26	.04	.29	.09	.04
SD ----------	(.000)	(.125)	(.121)	(.379)	(.259)	(.130)
S—						
Wt ----------	38.3	38.9	38.4	38.6	38.9	39.0
At ----------	52.43	52.64	52.13	52.63	52.69	52.57
SD ----------	(.135)	(.338)	(.930)	(.272)	(.163)	(.197)
Total (Wt) -------	98.83	99.89	99.78	99.24	99.69	99.84
Metals/S ----------	.907	.899	.918	.900	.898	.896

temperatures similar to those recorded in surrounding peridotites and in other ophiolites. The values obtained from these pyroxenes show temperatures of reequilibration, not the temperature of initial crystallization.

SUMMARY AND DISCUSSION

Rocks adjacent to the Illinois River host two distinctly different types of sulfides. Disseminated, net-textured, and massive sulfides composed principally of pyrrhotite, chalcopyrite, and cobalt-bearing pentlandite occur in relatively undeformed and unmetamorphosed pyroxene cumulates. The sulfides have textures and compositions typical of magmatic sulfide deposits. Ni/Cu and precious-metal patterns indicate that the sulfides equilibrated with gabbroic liquids. In contrast, metagabbroic rocks that show granulite-grade metamorphism and intense deformation contain stratabound stringers of pyrite-chalcopyrite mineralization.

Locally the sulfides have been remobilized during the faulting that juxtaposed the two rock types. This is most clearly shown by the pyrrhotite-rich sulfides that occur as massive pods near the fault, stringers in the fault, and injections into adjacent metagabbroic rocks. The chemical effect of remobilization has been to reduce the abundance of Ni, Cu, Co, and precious metals relative to Fe, to increase the amount of Co relative to Ni and Cu, and to form minor amounts of pentlandite that is very rich in cobalt. Although rocks adjacent to the fault appear unaltered, it is not known if this remobilization occurred solely as a result of deformation or if it also involved movement of fluids.

Whereas the pyroxenite appears to be relatively undeformed and unmetamorphosed, the adjacent metagabbroic rocks clearly have a complex history of granulite-grade metamorphism and intense deformation. Two environments for these events seem possible. High-temperature and low- to moderate-pressure metamorphic assemblages occur in dynamothermally metamorphosed rocks at the base of some

Table 10. Electron microprobe analyses of chalcopyrite
[Wt, weight percent; At, atomic percent; SD, standard deviation]

	Pyroxene cumulate				Metagabbroic sequence					
Sample number -------	250–2	250–3	251–3	253–3	245–1	246–1	251–4	252–1	253–1	253–2
Fe—										
Wt ----------	30.8	30.2	30.1	30.7	29.8	29.4	31.2	30.6	30.2	30.9
At ----------	25.22	24.72	24.75	25.06	24.47	24.25	25.3	25.2	24.87	25.13
SD ----------	(.477)	(.530)	(.629)	(.355)	(.827)	(.460)	(.143)	(.565)	(.361)	(.345)
Ni—										
Wt ----------	.13	.08	.03	.01	.45	.00	.21	.23	.11	.16
At ----------	.09	.05	.05	.00	.37	.00	.14	.18	.09	.14
SD ----------	(.115)	(.131)	(.072)	(.026)	(.636)	(.304)	(.189)	(.332)	(.163)	(.271)
Cu—										
Wt ----------	34.5	34.7	34.2	34.0	33.6	34.7	34.2	33.5	34.2	34.4
At ----------	24.80	24.95	24.70	24.41	24.25	25.17	24.47	24.25	24.69	24.02
SD ----------	(.465)	(.457)	(.848)	(.242)	(.714)	(.254)	(.892)	(.395)	(.226)	(.061)
Co—										
Wt ----------	.08	.21	.16	.05	.22	.00	.00	.00	.09	.13
At ----------	.05	.14	.14	.05	.18	.00	.00	.00	.05	.09
SD ----------	(.138)	(.244)	(.100)	(.126)	(.317)	(.000)	(.000)	(.000)	(.134)	(.219)
S—										
Wt ----------	35.0	35.2	35.2	35.5	35.5	35.2	35.4	35.1	35.1	35.3
At ----------	49.84	50.14	50.37	50.48	50.73	50.57	50.09	50.37	50.30	50.02
SD ----------	(.163)	(.356)	(.185)	(.242)	(.346)	(.353)	(.170)	(.184)	(.099)	(.244)
Total (Wt) ---------	100.51	100.39	99.69	100.26	99.57	99.30	101.01	99.43	99.7	100.89
Metal/S ----------	1.006	.995	.985	.981	.971	.977	.996	.985	.988	.999

Table 11. Electron microprobe analyses of pyrite
[Wt, weight percent; At, atomic percent; SD, standard deviation]

	Pyroxene cumulate		Metagabbroic sequence					
Sample number -----	250–3	253–3	245–1	246–1	251–4	252–1	253–1	253–2
Fe—								
Wt ----------	47.06	46.1	45.2	46.7	46.0	46.6	45.7	46.80
At ----------	33.30	33.15	32.24	32.99	32.91	33.13	32.89	33.4
SD ----------	(.200)	(.602)	(1.13)	(.687)	(.689)	(.145)	(.484)	(.501)
Ni—								
Wt ----------	.19	.95	.15	.14	.29	.05	.27	.02
At ----------	.13	.64	.08	.08	.20	.04	.20	.00
SD ----------	(.115)	(.545)	(.177)	(.170)	(.480)	(.100)	(.386)	(.061)
Cu—								
Wt ----------	.18	.05	.74	.00	.14	.00	.03	.02
At ----------	.12	.04	.48	.00	.08	.00	.00	.00
SD ----------	(.028)	(.123)	(1.48)	(.000)	(.107)	(.000)	(.065)	(.061)
Co—								
Wt ----------	.20	.22	.04	.01	.12	.08	.03	.11
At ----------	.13	.16	.04	.00	.08	.04	.00	.08
SD ----------	(.190)	(.404)	(.090)	(.144)	(.245)	(.700)	(.038)	(.133)
S—								
Wt ----------	53.81	52.7	54.1	54.4	53.51	53.9	53.3	53.4
At ----------	66.32	66.01	67.16	66.93	66.73	66.79	66.91	66.57
SD ----------	(.057)	(.150)	(.831)	(.128)	(.334)	(.198)	(.426)	(.249)
Total (Wt) --------	101.44	100.02	100.23	101.25	100.06	100.63	99.33	100.35
Metals/S ----------	.507	.515	.489	.494	.498	.497	.495	.503

ophiolites. However, these sequences are generally less than 1,000 m thick, are multiply deformed, and show closely spaced changes in metamorphic mineral assemblages that indicate presence of a steep thermal gradient in the past (Williams and Smyth, 1973; Malpas, 1979). These are features not apparent in the limited exposures of metagabbroic rock near this sulfide occurrence or in extensive exposures of similar rocks that make up the Big Craggies (fig. 1). Alternatively, these rocks may be part of a high-temperature, low-pressure metamorphic belt that formed near an island-arc complex (Miyashiro, 1973). Similarities in age and petrology between these rocks and those of the Chetco River complex, parts of which are considered to be part of an island arc (Nicholson, 1981), make this latter alternative attractive. Blueschist assemblages that are the same age as some of the younger metagabbroic rocks occur to the west (Coleman, 1972) and could represent the complimentary high-pressure low-temperature part of the paired metamorphic belt.

The study of the Illinois River sulfide occurrence was part of a larger program designed to evaluate the mineral-resource potential of this part of southwestern Oregon (Page and others, 1982). Although this sulfide is not economically significant, similar sulfide occurrences in adjacent parts of this ultramafic complex indicate that more economically significant sulfide concentrations might be found. However, the sulfides described here are more likely to be of interest because they represent a rare documentation of immiscible magmatic sulfides within a fragment of oceanic crust. This type of mineralization may also represent the primary concentration of metals that are remobilized and reconcentrated to make the Co-Ni-Cu arsenide and sulfide vein deposits found in many altered ophiolite complexes. Although not a well-known part of ophiolite metallogeny, vein deposits of this type are found in the Mackinaw Mine, Washington (Milton and Milton, 1959), Mesozoic ophiolites in Italy (Zuffardi, 1977), the West Carpathians (Hovorka and Ivan, 1980), the Proterozoic ophiolite at Bou Azzer, Morocco

Table 12. Compositions of five sulfide-bearing samples, whole-rock analyses

[Co, Cu, and Ni were determined by flame atomic absorption, and total sulfur was obtained by an infrared sulfur determinator (analyses made in USGS laboratory; M.W. Doughten, analyst). Platinum group metals (PGM's) and Au were determined by means of a fire assay-spectrographic method (USGS laboratory; R.R. Carlson and E.F. Cooley, analysts)]

Sample number	Ni (ppm)	Cu (ppm)	Co (ppm)	S (percent)	Pt (ppm)	Pd (ppm)	Rh (ppm)	Au (ppm)	S/Ni	Ni/Cu	Ni/Co
250–2	740	3,400	130	1.8	0.150	0.500	0.002	0.700	23.3	0.22	5.7
250–3	420	1,600	270	10.7	.150	.500	<.002	.150	254.7	.26	1.5
251–3	310	1,600	76	.53	.150	.300	<.002	.100	17.1	.19	4.1
253–3	700	4,900	340	7.6	.150	.300	<.002	.200	108.5	.14	2.1
251–4	220	2,400	130	5.9	.050	.200	<.002	.200	268.2	.092	1.7

Table 13. Compositions of five sulfide-bearing samples, analyses recalculated to 100 percent sulfide

Sample number	Fe (weight percent)[1]	Ni (weight percent)[1]	Cu (weight percent)[1]	Co (weight percent)[1]	S (weight percent)[1]	Pt (ppm)	Pd (ppm)	Rh (ppm)	Au (ppm)
250–2	53.2	1.5	7.1	0.3	37.8	3.15	10.5	0.042	14.72
	(41.8)	(1.1)	(4.9)	(.2)	(51.8)				
[2]250–3	59.1	.1	.6	.1	40.1	.568	1.878	<.007	.568
	(45.6)	(.1)	(.4)	(.1)	(53.8)				
251–3	48.6	2.2	11.6	.5	37.1	10.4	20.9	<.139	6.98
	(38.6)	(1.7)	(8.1)	(.4)	(57.2)				
[2]253–3	56.9	.4	2.5	.2	39.9	.767	1.53	<.010	1.023
	(44.2)	(.3)	(1.7)	(.1)	(53.8)				
[3]251–4	58.1	.1	1.6	.08	40.0	.330	1.320	<.013	1.320
	(44.9)	(.1)	(1.0)	(.0)	(53.84)				

[1]Atomic percent is in parentheses.
[2]Based on pyrite/pyrrohotite = 1/15.
[3]Based on pyrite/pyrrhotite = 1/10.

Table 14. Metal-metal and metal-sulfur ratios from recalculated 100 percent sulfide compositions

	Disseminated sulfides		Interconnected sulfides		
Sample number	250–2	251–3	250–3	253–3	251–4
Ni/Cu	0.21	0.19	0.18	0.16	0.06
Ni/Co	5.00	4.40	1.10	2.00	1.25
Pt/Pd	.30	.49	.29	.50	.25
Pt/Au	.21	1.49	1.00	7.50	.25
(Fe+Ni+Cu+Co)/S	1.64	1.69	1.49	1.50	1.50
Fe/S	1.41	1.31	1.47	1.43	1.45
Fe/Ni+Cu+Co	5.98	3.40	73.8	18.3	32.6

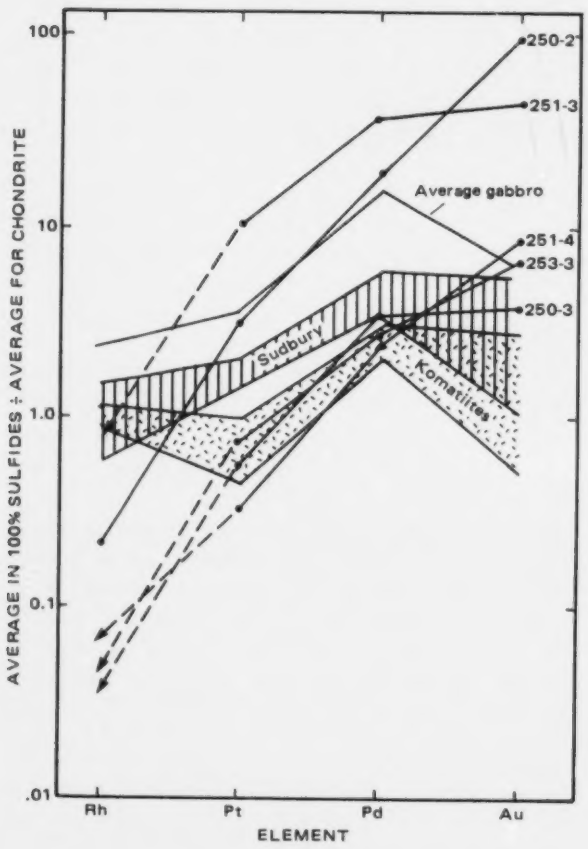

Figure 5. Chondrite-normalized plot of PGM (platinum group metals) and Au contents after recalculation to 100 percent sulfides. Also shown are fields determined by Naldrett (1981) for komatiites, Sudbury ores, and average pattern of several gabbro-hosted sulfide deposits. Detection limits greater than the amount of Rh present are shown by dashed line and arrow.

(Leblanc, 1975, 1981), and in the Limmasol Forest Plutonic Complex, Cyprus (Panayiotou, 1980). Of these occurrences, the one at Bou Azzer, Morroco, is the most significant and, in fact, until recently was the only deposit where cobalt was mined as the principal product.

The well-documented arsenide mineralization in part of the Limmasol Forest Plutonic Complex, Cyprus, has particular bearing on this type of mineralization. This complex, which is part of the Trodoos ophiolite, contains two separate mineralized areas (Panayiotou, 1980). Both have sulfides and arsenides (mostly monoclinic pyrrhotite, chalcopyrite, cubanite, and loellingite in the first area, and troilite, valleriite, maucherite, chalcopyrite, and pentlandite in the second) that are concentrated in veins and fractures. Most of the mineralization is near the contact between wehrlite and harzburgite and is believed to result from arsenic-bearing fluids that remobilized magmatic sulfides during serpentinization (Panayiotou, 1980). Small amounts of disseminated sulfides occur above the ore zone and are described as drops of an immiscible sulfide liquid that formed the initial deposit and were subsequently remobilized and altered by the arsenic-bearing fluids.

The sulfides in the nearly unserpentinized cumulates along the Illinois River may, therefore, represent the protore from which the mineralization in the Limmasol Forest Plutonic Complex formed. Although the processes by which the secondary vein deposits form, and particularly the source of the arsenic-bearings fluids, are not well established, the metals in these deposits were probably moved by arsenic-bearing fluids, which were derived from outside sources and were introduced during serpentinization and shearing (Zuffardi, 1977; Leblanc, 1975; Panayiotou, 1980). Regardless of the process, the chemical and mineralogical alteration observed in the cumulate-hosted sulfides along the Illinois River show that mobilization of Cu, Ni, Co, and precious metals occurred.

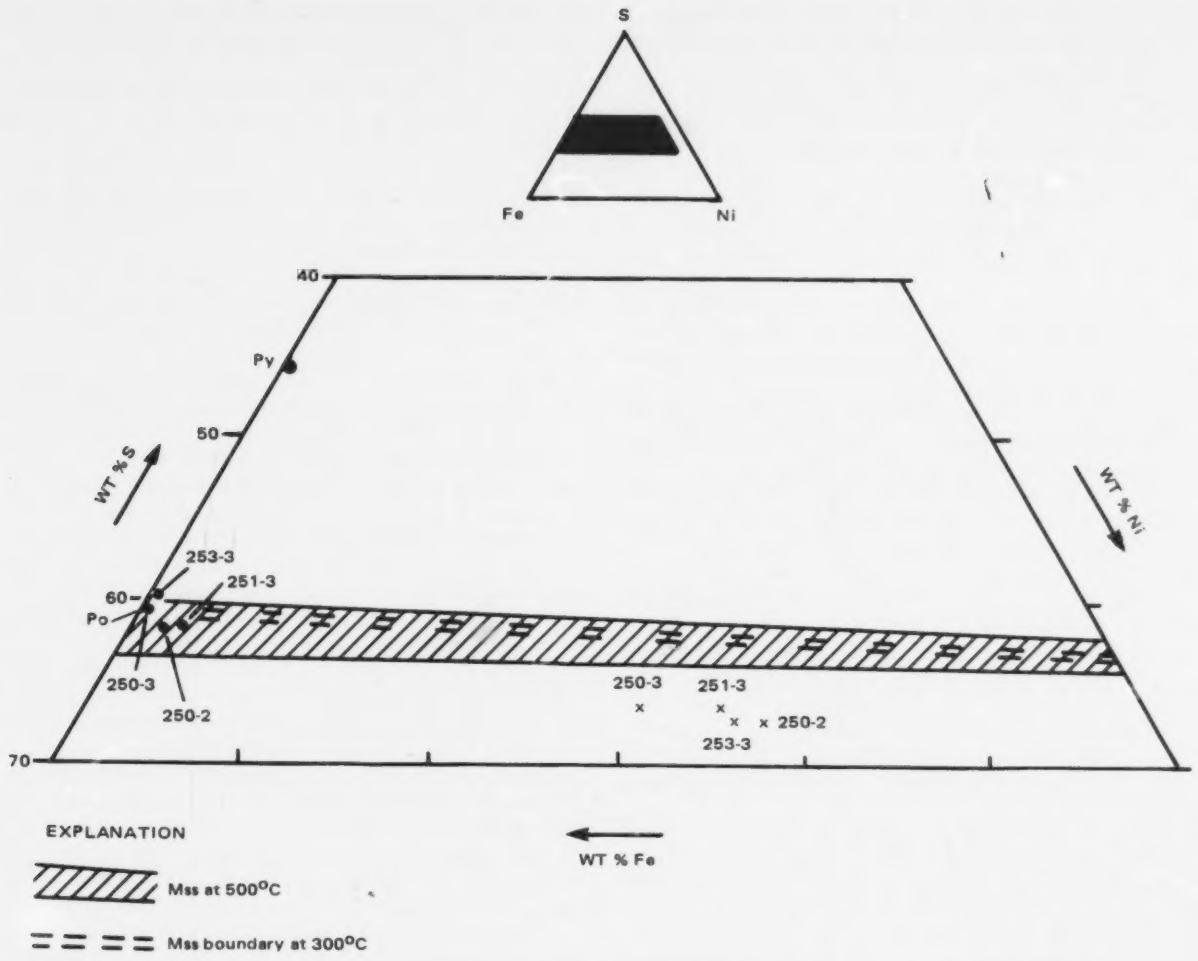

Figure 6. Composition of sulfides from cumulus pyroxenite plotted on the Fe-Ni-S diagram. For this diagram, proportional amounts of cobalt have been added to nickel and iron; the compositions of 100 percent sulfides from table 13 have been further modified by removing the metals and sulfur present as chalcopyrite. X, compositions of pentlandites; Po and Py, fields of pyrrhotite and pyrite compositions.

REFERENCES CITED

Albee, A.L., and Ray, Lily, 1970, Correction factors for electron probe microanalysis of silicates, oxides, carbonates, phosphates, and sulfates: Analytical Chemistry, v. 42, p. 1408–1414.

Bailey, E.H., Blake, M.C., Jr., Jones, D.L., 1970, On-land Mesozoic oceanic crust in California Coast Ranges, *in* Geological Survey Research 1970: U.S. Geological Survey Professional Paper 700–C, p. C70–C81.

Bence, A.E., and Albee, A.L., 1968, Empirical correction factors for electron microanalysis of silicate and oxides: Journal of Geology, v. 76, p. 382–403.

Bohlen, S.R., and Essene, E.J., 1979, A critical evaluation of two-pyroxene thermometry in Adirondack granulites: Lithos, v. 12, no. 4, p. 335–345.

Burchfiel, B.C., and Davis, G.A., 1975, Nature and controls of Cordilleran orogenesis, western United States; extension of an earlier synthesis: American Journal of Science, v. 275–A, p. 363–396.

Coleman, R.G., 1972, The Colebrooke Schist of southwestern Oregon and its relation to the tectonic evolution of the region: U.S. Geological Survey Bulletin 1339, 61 p.

——— 1977, Ophiolites: Berlin, Springer-Verlag, 229 p.

Craig, J.R., and Scott, S.D., 1974, Sulfide phase equilibria, *in* Ribbe, P.H., ed., Sulfide mineralogy: Mineralogical Society of America, Short Course Notes, p. CS1–CS110.

Dick, H.J.B., 1977, Partial melting in the Josephine Perdotite I, the effect of mineral composition and its consequence for geobarometry and geothermometry: American Journal of Science, v. 277, no. 7, p. 801–832.

Diller, J.S., 1907, The Mesozoic sediments of southwestern Oregon: American Journal of Science, ser. 4, v. 23, p. 401–421.

Dott, R.H., 1965, Mesozoic-Cenozoic tectonic history of the southwest Oregon coast in relation to Cordilleran orogenesis: Journal of Geophysical Research, v. 70, p. 4687–4708.

Duke, J.M., 1979, Computer similation of the fractionation of olivine and sulfide from mafic and ultramafic magmas: Canadian Mineralogist, v. 17, p. 507–514.

Duke, J.M., and Naldrett, A.J., 1978, A numerical model of the fractionation of olivine and molten sulfide from a komatiite magma: Earth and Planetary Science Letters, v. 39, no. 2, p. 255–266.

England, R.N., and Davies, H.L., 1973, Mineralogy of ultramafic cumulates and tectonites from eastern Papua: Earth and Planetary Science Letters, v. 17, no. 2, p. 416–425.

Evarts, R.C., 1977, The geology and petrology of the Del Puerto ophiolite, Diablo Range, central California Coast ranges, *in* Coleman, R.G., and Irwin, W.P., eds., North American Ophiolites: Oregon Department of Geology and Mineral Industries Bulletin 95, p. 121–139.

Garcia, M.O., 1979, Petrology of the Rogue and Galice Formations, Klamath Mountains, Oregon: Identification of a Jurassic island arc sequence: Journal of Geology, v. 87, p. 29–41.

George, R.P. Jr., 1978, Structural petrology of the Olympus ultramafic complex in the Troodos ophiolite, Cyprus: Geological Society of America Bulletin, v. 89, p. 845–865.

Gray, Floyd, 1980, Geology of the igneous complex at Tin Cup Peak, Kalmiopsis Wilderness Area, southwestern Oregon: U.S. Geological Survey Open File Report 80–1243, 72 p.

Harper, G.D., 1979, "Anomalous" ophiolite underlying late Jurassic metasedimentary rocks of the Galice Formation, western Jurassic belt, northwestern California [abs.]: Geological Society of America Abstracts with Programs, v. 11, no. 3, p. 82.

——— 1980, The Josephine Ophiolite; remains of Late Jurassic marginal basin in northwestern California: Geology, v. 8, no. 7, p. 333–337.

Harper, G.D., and Saleeby, J.B., 1980, Zircon ages of the Josephine Ophiolite and the Lower Coon Mountain Pluton, western Jurassic belt, northwestern California [abs.]: Geological Society of America Abstracts with Programs, v. 12, no. 3, p. 109–110.

Harris, D.C., and Nickel, E.H., 1972, Pentlandite compositions and associations in some mineral deposits: Canadian Mineralogist, v. 11, p. 861–878.

Henry, D.J., and Medaris, L.G., Jr., 1980, Application of pyroxene and olivine-spinel geothermometers to peridotites in southwestern Oregon: American Journal of Science, v. 280–A, p. 211–231.

Henson, B.J., and Green, D.H., 1972, Experimental study of the stability of cordierite and garnet in pelitic compositions at high pressure and temperatures. II, Compositions without excess alumino silicates: Contributions to Mineralogy and Petrology, v. 25, p. 331–354.

Himmelberg, G.R., and Loney, R.A., 1973, Petrology of the Vulcan Peak alpine-type peridotite, southwestern Oregon: Geological Society of America Bulletin, v. 84, p. 1585–1600.

——— 1980, Petrology of ultramafic and gabbroic rocks of the Canyon Mountain ophiolite, Oregon: American Journal of Science, v. 280–A, p. 232–268.

Hopson, C.A., and Frano, C.J., 1977, Igneous history of the Point Sal ophiolite, southern California, *in* Coleman, R.G., and Irwin, W.P., eds., North American ophiolites: Oregon Department of Geology and Mineral Industries Bulletin 95, p. 161–183.

Hotz, P.F., 1971, Plutonic rocks of the Klamath Mountains, California and Oregon: U.S. Geological Survey Professional Paper 684–B, p. B1–B20.

Hovorka, Dusan, and Ivan, Peter, 1980, A hydrothermal leaching of an ultrabasic body—a determinant phenomenon of the Co-Ni arsenide vein deposit genesis (Dobsina, the West Carpathians), *in* UNESCO, an International Symposium on Metallogeny of Mafic and Ultramafic Complexes; the eastern Mediterranean-western Asia area, and its comparison with similar metallogenic environments in the world [abs.]: Athens, Greece, p. 172–184.

Huhma, M., 1970, Nickel, cobalt, and copper in some rocks in the Outokumpu region: Bulletin of the Geological Society of Finland, v. 42, p. 67–88.

Irwin, W.P., 1964, Late Mesozoic orogenies in the ultramafic belts of northwestern California and southwestern Oregon, *in* Geological Survey Research 1964: U.S. Geological Survey Professional Paper 501–C, p. C1–C9.

——— 1966, Geology of the Klamath Mountain province, *in* Bailey, E.H., ed., Geology of northern California: California Divison of Mines and Geology Bulletin 190, p. 19–38.

——— 1977, Ophiolite terranes of California, Oregon, and Nevada, *in* Coleman, R.G., and Irwin, W.P., eds., North American ophiolites: Oregon Department of Geology and Mineral Industries Bulletin 95, p. 75–92.

Jackson, E.D., Green, H.W., II, Moores, E.M., 1975, The Vourinos Ophiolite, Greece: Cyclic units of lineated cumulates overlying harzburgite tectonite: Geological Society of America Bulletin, v. 86, no. 3, p. 390–398.

Juteau, T., and Whitechurch, H., 1980, The magmatic cumulates of Antalya (Turkey); evidence of multiple intrusions in an ophiolitic magma chamber, *in* Panayiotou, A., ed., Ophiolites: International Ophiolite Symposium, Cyprus, 1979, Proceedings, p. 377–391.

Kouvo, O., Huhma, M., and Vuorelainen, Y., 1959, A natural cobalt analogue of pentlandite: American Mineralogist, v. 44, p. 897–900.

Kullerud, G., Yund, R.A., and Moh, G.H., 1969, Phase relations in the Cu-Fe-S, Cu-Ni-S, and Fe-Ni-S systems, *in* Wilson, H.D.B., and Bateman, A.M., eds., Magmatic ore deposits, a symposium [Stanford Univ., 1966]: Economic Geology Monograph 4, p. 323–343.

Laurent, Roger, 1977, Ophiolities from the northern Appalachians of Quebec, *in* Coleman, R.G., and Irwin, W.P., eds., North American ophiolites: Oregon Department of Geology and Mineral Industries Bulletin 95, p. 25–40.

Leblanc, Marc, 1975, Ophiolites précambriennes et gîtes arséniés de cobalt (Bou Azzer-Maroc): Centre Géologique et Géophysique Montpellier, France, Memoire Mois-Series, 329 p.

——— 1981, Ophiolites précambriennes et gîtes arséniés de cobalt (Bou Azzer-Maroc): Notes et Memoires du Service Geologique du Maroc, no. 280, 306 p.

Leblanc, Marc, and Billaud, P., 1982, Cobalt arsenide ore bodies related to an upper Proterozoic ophiolite, Bou Azzer (Morocco): Economic Geology, v. 77, p. 162–175.

Loney, R.A., and Himmelberg, G.R., 1976, Structure of the Vulcan Peak alpine-type peridotite, southwest Oregon: Geological Society of America Bulletin, v. 87, p. 259–274.

——— 1977, Geology of the gabbroic complex along the northern border of the Josephine peridotite, Vulcan Peak area, southwestern Oregon: U.S. Geological Survey Journal of Research, v. 5, no. 6, p. 761–781.

Malpas, J., 1979, The dynamothermal aureole of the Bay of Islands ophiolite suite: Canadian Journal of Earth Science, v. 16, p. 2086–2101.

Matsuhara, S. and Kato, A., 1979, The occurrence of heazlewoodite and cobalt pentlandite from the Nakauri mine, Aich; Pretecture, Japan: Tokyo, Memoir of the National Science Museum, no. 12, p. 3–11.

Medaris, L.G., Jr., 1972, High-pressure peridotites in southwestern Oregon: Geological Society of America Bulletin, v. 83, p. 41–58.

Milton, Charles, and Milton, D.J., 1959, Nickel-gold ore of the Mackinaw mine, Snohomish County, Washington: Economic Geology, v. 53, p. 426–447.

Misra, K.C., and Fleet, M.E., 1973, The chemical compositions of synthetic and natural pentlandite assemblages: Economic Geology, v. 68, p. 518–539.

Miyashiro, A., 1973, Metamorphism and metamorphic belts: New York, John Wiley and Sons, 492 p.

Morgan, B.A., 1977, The Baltimore Complex, Maryland, Pennsylvania, and Virginia, *in* Coleman, R.G., and Irwin, W.P., eds., North American ophiolites: Oregon Department of Geology and Mineral Industries Bulletin 95, p. 41–49.

Naldrett, A.J., 1973, Nickel sulfide deposits—their classification and genesis, with special emphasis on deposits of volcanic association: CIM Bulletin, November 1973, p. 45–63.

——— 1979, Partitioning of Fe, Co, Ni, Cu between sulfide liquid and basaltic melts and the composition of Ni-Cu sulfide deposits—A reply and further discussion: Economic Geology, v. 74, p. 1520–1528.

——— 1981, Nickel sulfide deposits: Classification, composition, and genesis: Economic Geology 75th Anniversary Volume, p. 628–685.

Naldrett, A.J., and Cabri, L.J., 1976, Ultramafic and related mafic rocks: Their classification and genesis with special reference to the concentration of nickel sulfides and platinum-group elements: Economic Geology, v. 71, p. 1131–1158.

Naldrett, A.J., Craig, J.R., and Kullerud, G., 1967, The central portion of the Fe-Ni-S system and its bearing on pentlandite exsolution in iron-nickel sulfide ores: Economic Geology, v. 62, p. 826–847.

Naldrett, A.J., Hoffman, E.L., Green, A.H., Chou, G., and Naldrett, S.R., 1979, The composition of Ni-sulfide ores, with particular reference to their content of PGE and Au: Canadian Mineralogist, v. 17, p. 403–415.

Nicholson, S.W., 1981, Petrography and geochemistry of the Illinois River Gabbros, Kalmiopsis Wilderness Area, southwestern Oregon: University of Massachusetts unpublished M.S. thesis, 137 p.

Page, N.J, Gray, Floyd, Cannon, J.K., Foose, M.P., Lipin, B.R., Moring, B.C., Nicholson, S.W., Sawlin, M.G., Till, Alison, and Ziemianski, W.P., 1981, Geologic Map of the Kalmiopsis Wilderness Area, Oregon: U.S. Geological Survey Miscellaneous Field Studies Map MF–1240–A.

Page, N.J, Grimes, D.J., Leinz, R.W., Blakely, R.W., Lipin, B.R., Foose, M.P., Gray, Floyd, 1982, Mineral resource potential map of the Kalmiopsis Wilderness, southwestern Oregon: U.S. Geological Survey Miscellaneous Field Studies Map MF–1240–E.

Page, N.J, Moring, Barry, Gray, Floyd, Cannon, Jerome, and Blair, W.N., 1981, Reconnaissance geologic map of the Selma quadrangle, Josephine County, Oregon: U.S. Geological Survey Miscellaneous Field Studies Map, MF–1349.

Panayiotou, A., 1980, Cu-Ni-Co-Fe sulfide mineralization, Limassol Forest, Cyprus, *in* Panayiotou, A., ed., Ophiolites: International Ophiolite Symposium, Cyprus, 1979, Proceedings, p. 102–116.

Papike, J.J., Cameron, K.L., and Baldwin, K., 1974, Amphiboles and pyroxenes: Characterization of *other* than quadrilateral components and estimates of ferric iron from microprobe data [abs.]: Geological Society of America Abstracts with Programs, v. 6, no. 7, p. 1053–1054.

Parks, H.M., and Swartley, A.M., 1916, The mineral resources of Oregon: Oregon Bureau of Mines and Geology, Resources of Oregon, v. 2, no. 4, p. 57.

Petruk, W., Harris, D.C., and Stewart, J.M., 1969, Langisite, a new mineral, and the rare minerals cobalt pentlandite, siegenite, parkerite, and bravoite from the Langis mine, Cobalt-Gowganda area, Ontario: Canadian Mineralogist, v. 9, pt. 5, p. 597–616.

Ramp, Len, 1964, Geologic adventures on the lower Illinois River, southwestern Oregon: Ore Bin, v. 26, no. 6, p. 97–108.

——— 1969, Dothan(?) fossils discovered: Ore Bin, v. 31, no. 12, p. 245–246.

——— 1975, Geology and mineral resources of the upper Chetco drainage area, Oregon, including the Kalmiopsis Wilderness and Big Craggies Botanical areas: Oregon Department of Geology and Mineral Industries Bulletin 88, 47 p.

Ramp, Len, Schlicker, H.G., and Gray, J.J., 1977, Geology, mineral resources and rock material of Curry County, Oregon: Oregon Department of Geology and Mineral Industries Bulletin 93, 79 p.

Simkin, Tom, and Smith, J.V., 1970, Minor-element distribution in olivine: Journal of Geology, v. 78, p. 304–325.

Thayer, T.P., 1980, Syncrystallization and subsolidus deformation in ophiolitic peridotite and gabbro: American Journal of Science, v. 280–A, p. 269–283.

Wells, F.G., Hotz, P.E., and Cater, F. W., Jr., 1949, Preliminary description of the geology of the Kerby Quadrangle, Oregon: Oregon Department of Geology and Mineral Industries Bulletin 40, 23 p.

Wells, P.R.A., 1977, Pyroxene thermometry in simple and complex systems: Contributions to Mineralogy and Petrology, v. 62, p. 129–139.

Williams, H., and Smyth, W.R., 1973, Metamorphic aureoles beneath ophiolite suites and alpine peridotites; tectonic implications with west Newfoundland examples: American Journal of Science: v. 273, p. 594–621.

Winkler, Helmut G.F., 1967, Petrogenesis of metamorphic rocks: New York, Springer-Verlag, 237 p.

Zuffardi, P., 1977, Ore mineral deposits related to the Mesozoic ophiolites in Italy, *in* Klemm, D.D., and Schneider, H.J., eds., Time and strata-bound ore deposits: New York, Springer-Verlag, p. 314–323.